

Optimizing Analog Filter Designs for Minimum Nonlinear Distortions Using Multisine Excitations

J. Lataire⁽¹⁾, G. Vandersteen^(2,1), R. Pintelon⁽¹⁾

(1) Vrije Universiteit Brussel, Department ELEC, Pleinlaan 2, B1050 Brussels, Belgium, email: jlataire@vub.ac.be
(2) IMEC vzw, Kapeldreef 75, B3001 Leuven, Belgium

Abstract

Nonlinear distortions in submicron analog circuits are gaining importance, especially when power constraints are imposed and when operating in moderate inversion. This paper proposes a method to optimize the design of analog filters for minimum noise and nonlinear distortions. For this purpose a technique is presented for quantifying these nonlinearities, such that their influence can be compared with that of the system noise. Having quantified the non-idealities, an optimization can be carried out which involves the tuning of design parameters.

1. Introduction

Multi-objective optimization is often used during the design of analog circuits [1][2]. Objective functions can be defined in various ways. In this paper the *deviation of the transfer function w.r.t. a desired characteristic*, the *nonlinear distortions* and the *system noise* of analog active filters are considered. For dominantly linear systems, such as amplifiers and filters, it is possible to interrelate the nonlinearities and the system noise and to deduce a total distortion-to-signal ratio. An obvious advantage of this interrelation is the reduction of the number of objectives in the optimization.

Nonlinear distortions are classically extracted using intercepts or compression points. However if the nonlinear distortions become frequency dependent (such as in e.g. filters) then the intercept points will also vary with the frequency. Hence, it is dangerous to use a single number for characterizing the nonlinear distortions of the circuit.

The proposed method for quantifying the nonlinearities is based on the analysis of circuits using random phase multisine excitations. The advantages are:

1. A multisine signal can be made such that it resembles the final signal used. As a consequence, it allows the designer to predict the actual impact of nonlinear distortions, given the characteristics of the signal that will be applied to the circuit.
2. The sources of the nonlinear distortions can be identified.
3. The nonlinear distortions can be split up in a deterministic and a stochastic part. The deterministic part is

responsible for a bias contribution on the transfer function. The stochastic part acts as an additive noise source on the transfer function. This noise source has a lot in common with the system noise.

This paper is organized as follows. First it will be shown how to quantify the considered performances (non-idealities) using multisine excitations (section 2) and how to translate them in a multi-objective optimization problem (section 3). In section 4 the optimization procedure is applied to two filter topologies in order to extract the Pareto-optimal fronts for the trade-off between the (frequency dependent) linear and nonlinear distortions. Section 5 concludes.

2. Quantification of the non-idealities

The initial design of an analog active filter assumes that the basic building blocks behave ideally. OTA's (Operational Transconductance Amplifiers) are supposed to be linear with an infinite bandwidth, capacitors should be purely capacitive, ... Any deviation from this ideal behavior will therefore cause distortions. A distinction can be made between linear distortions, nonlinear distortions and system noise.

2.1. Linear distortions

Examples of linear distortions are readily found. The limited bandwidth of an OTA and the resistive loss of a capacitor are two examples of non-idealities that induce errors in the desired transfer function without introducing extra harmonics or other nonlinear effects. Considering these non-idealities in the initial design of a filter is a time-consuming job. Nevertheless those deficiencies can usually be compensated by tuning the parameters using a simple simulation-based optimization algorithm.

2.2. Nonlinear distortions

Basic building blocks of analog filters (operational amplifiers, ota's, resistors, capacitors, ...) are assumed to be dominantly linear. Nonlinearities are therefore, just like system noise, considered as a disturbance. This is why a quantification allowing to compare the influence of nonlinearities with that of system noise would be desirable. This can be achieved by using the approach introduced in [3]. This study gives the theoretical background (based on Volterra theory) for modelling a class of nonlinear systems in a simple manner. This class includes so-called weak non-

Acknowledgement: This work is sponsored by the Fund for Scientific Research (FWO-Vlaanderen), the Flemish Government (GOA-IMMI) and the Belgian Federal Government (IUAP VI)

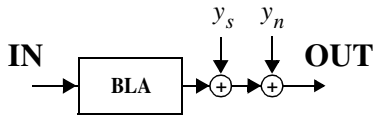


Fig. 1 Modelling of a weakly nonlinear system as a BLA and two additive noise sources

linearities (e.g. compression) as well as strong nonlinearities (e.g. relays, saturation, ...) but doesn't include bifurcations and chaos. This section summarizes the relevant aspects of [3] for this paper and considers their practical implementation for simulated electronic circuits.

As illustrated in Fig. 1, a nonlinear system is modelled as a "Best Linear Approximation" (BLA) with on the output two noise contributions y_s and y_n , both computable with existing simulators.

- The *BLA* is by definition the (hypothetical) linear system which predicts the best the output signal in least square sense for a given class of input signals. This class of a signal is determined by its power spectrum and its probability density function (pdf). It can be shown [3] that the BLA of a nonlinear system equals:

$$G_{BLA}(s) = G_o(s) + G_B(s) \quad (1)$$

(in the Laplace domain) where $G_o(s)$ is the true underlying linear system (or AC equivalent) and where $G_B(s)$ is a bias term depending on the class of the input signals and the odd nonlinearities. $G_B(s)$ is determined by the deterministic nonlinear contributions, as explained further. The BLA of a (weakly) nonlinear electronic circuit hence depends on the pdf and the power spectrum of the input signal used. A motivation to prefer the BLA over the AC-equivalent is that the former takes nonlinearities into account and thus will give a better prediction of the output signal.

- The *distortions due to nonlinearities* y_s (also known as stochastic nonlinear contributions) are noise contributions calculated with a time-domain analysis (transient analysis) or a frequency domain method. They have a lot in common with system noise, if some weak assumptions on the excitation signals are satisfied [3].
- The *System noise* y_n (thermal, flicker, ...) can be determined with a NOISE analysis (see section 2.3).

The BLA and the stochastic contributions of nonlinearities are calculated using one and the same time- or frequency-domain analysis. A well-chosen excitation signal is applied to the filter in this analysis, namely a random phase multisine, which is mathematically expressed as:

$$u(t) = \sum_{\kappa} A_{\kappa} \sin(2\pi\kappa f_o t + \varphi_{\kappa}) \quad (2)$$

where the κ 's are - not necessarily consecutive - natural numbers. The phases φ_{κ} are stochastic variables w.r.t. κ and are uniformly distributed between 0 and 2π (note that

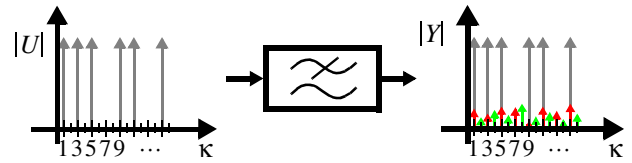


Fig. 2 Detection of nonlinearities using multisine excitations. A distinction has been made between linear contributions (grey) odd nonlinear contributions (red) and even nonlinear contributions (green)

φ_{κ} is constant with time). The signal $u(t)$ has (in good approximation) a normal distribution (so the pdf is known) and a power spectrum that can be chosen arbitrarily by varying the values of the amplitudes A_{κ} . From (2) it is also clear that this signal is composed of frequency components (so-called excited lines), which are all multiples of f_o , called the fundamental frequency. Note that f_o determines the frequency resolution of the multisine and that the choices of the κ 's in combination with f_o determine the frequency band to be analyzed. If this signal is applied on a linear system, the energy on a frequency line of the resulting output signal will entirely originate from that same frequency line at the input signal. This will not be the case with nonlinear systems. For the considered class of systems, theory predicts that the output signal will contain energy contributions on every line whose frequency can be obtained by multiple sums of combinations of the frequencies of the excited lines. This is illustrated in Fig. 2, where the linear contributions are represented by grey arrows and the nonlinear contributions by the green and red arrows (respectively even and odd nonlinearities [3]). A distinction can be made between the deterministic and the stochastic nonlinear contributions.

- The *deterministic nonlinear contributions* have a fixed phase difference with the linear contribution and, as a consequence, will not cancel out after averaging. They contribute to $G_B(s)$ in (1).
- The *stochastic nonlinear contributions* have the property that, for each realization, their phases vary randomly w.r.t. the phase of the linear contribution. It can be shown that these nonlinear contributions will cancel out when averaged over a great number of realizations of the phases φ_{κ} . These stochastic nonlinear contributions are the cause of y_s in Fig. 1.

As suggested, the BLA of a filter can be calculated by applying different (say M) realizations of a multisine on the filter and by averaging the obtained Frequency Response Functions (FRF) over the M realizations. The FRF (for realization m) and the BLA on frequency line κ are estimated as:

$$\hat{FRF}_m(\kappa) = \frac{Y_m(\kappa)}{U_m(\kappa)} \quad (3)$$

$$\hat{G}_{BLA}(\kappa) = \frac{1}{M} \sum_{m=1}^M \hat{FRF}_m(\kappa) \quad (4)$$

where $Y_m(\kappa)$ and $U_m(\kappa)$ are the DFT's of one period of the steady-state response of respectively the output and input signals. Note that in (4) the influence of the deterministic contributions of the nonlinear distortions is taken into account.

As mentioned above, stochastic nonlinear contributions behave as additive noise on the output signal and correspond to y_s . Its variance can be calculated using the variance on the BLA (for convenience, parameter κ has been left out):

$$\hat{\sigma}_{BLA}^2 = \frac{1}{(M-1)M} \sum_{m=1}^M \|\hat{G}_{BLA} - FRF_m\|^2 \quad (5)$$

$$\hat{\sigma}_s^2 = M \|U_m\|^2 \hat{\sigma}_{BLA}^2 \quad (6)$$

The last equation gives the total amount of energy due to distortion in a frequency band centered around κf_o and with bandwidth f_o (f_o corresponding to the frequency resolution of the multisine). Note that, since the detection is performed using a periodic signal, the distortion is also periodic (as illustrated by the arrows on Fig. 3), in contrast with the system noise y_n as explained in section 2.3.

One issue about the detection of nonlinearities using multisines is the needed simulation time for the transient analysis. Since we are using a periodic signal, simulating a whole period of the steady-state response to the multisine would be convenient. The period of the multisine equals $1/f_o$, and hence, the higher the desired frequency resolution is, the longer the simulation time. The sampling frequency (and time step) depend on the desired accuracy [4]. As a rule of thumb they should be chosen such as to simulate at least 10 points of the highest excited frequency component. This should be done to avoid aliasing from higher harmonics. From this it follows that $10 \times \kappa_{max}$ time points in steady-state should be simulated. One could notice that the time domain simulation of a two-tone analysis performed at frequencies $(\kappa_{max}-1)f_o$ and $\kappa_{max}f_o$ would require the same amount of simulation points. The advantage of a multisine analysis is, however, that a lot more information is acquired.

Note that a shooting method (e.g. a Periodic Steady-State simulation) would provide the same results. However it has been experienced that this analysis is usually slower and

requires more memory to be carried out, especially for large filter circuits. The use of harmonic balance is dissuaded because of the great amount of nodes in a typical active filter and the great number of frequency lines of the multisine.

By following the methodology described in this section, one can predict the impact of the nonlinearities and define a so-called signal-to-distortion ratio for a given class of signals. Using a frequency resolution f_o that is small enough w.r.t. the analyzed frequency band, the smooth variations of the nonlinear distortions with the frequency become clearly visible.

2.3. System noise versus stochastic nonlinearities

Section 2.2 determines the noise due to stochastic nonlinear distortions. System noise, such as thermal noise and flicker noise, can be computed using the NOISE analysis of a circuit simulator. An important issue to consider when optimizing both the system noise and the nonlinear distortions is to compare them in a pragmatic way. It is important that one can determine whether or not the nonlinear distortions are significantly higher than the system noise. It would be pointless to minimize the system noise if the output signal would mainly be distorted by nonlinearities and vice versa.

The NOISE analyses allows one to determine the Power Spectral Density (PSD) of the different noise sources (expressed in V^2/Hz for instance and in Fig. 3 represented by the continuous stripe). The quantification method for the stochastic nonlinear distortion introduced in section 2.2 gives the total amount of distortion energy in a frequency band with a width of f_o , and is therefore expressed in V^2 . Consequently, the noise contributions should be denormalized. This can be carried out by integrating the PSD of the system noise over one frequency band. If the frequency resolution of the multisine is chosen such that the PSD stays nearly constant over a frequency band, then this can be approximated by:

$$\sigma_n^2(\kappa) = \int_{\kappa f_o - \frac{f_o}{2}}^{\kappa f_o + \frac{f_o}{2}} PSD_n(f) df \cong PSD_n(\kappa f_o) f_o \quad (7)$$

2.4. Deviation w.r.t. the desired transfer function

This far we have quantified both distortion contributions y_s and y_n in Fig. 1. An optimization algorithm should take into account the deviation of the realized transfer function w.r.t. the desired transfer function. As mentioned in section 2.2, the best estimation we have for this transfer function is the BLA. Hence, a possible quantification for the deviation is a normalized difference:

$$\hat{C}_{dev} = \sum_{\kappa} \frac{\|G_{des}(\omega_{\kappa}) - \hat{G}_{BLA}(\kappa)\|^2}{\|G_{des}(\omega_{\kappa})\|^2} w_{dev}(\omega_{\kappa}) \quad (8)$$

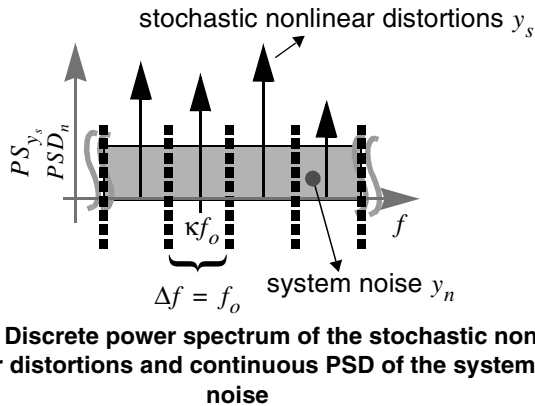


Fig. 3 Discrete power spectrum of the stochastic nonlinear distortions and continuous PSD of the system noise

with

- G_{des} the desired transfer function
- $\omega_\kappa = 2\pi\kappa f_o$
- w_{dev} a weighting function that should allow the designer to favour some frequency bands over others.

A regularization should be carried out if G_{des} includes transmission zeros to avoid bad conditioning around those points. Note that (8) can be written as

$$\hat{C}_{dev} = e_{dev}^H e_{dev} \quad (9)$$

$$e_{dev} = \begin{bmatrix} e_{dev, \kappa_1} \\ \dots \\ e_{dev, \kappa_n} \end{bmatrix}$$

$$e_{dev, \kappa} = \frac{G_{des}(\omega_\kappa) - G_{BLA}(\kappa)}{G_{des}(\omega_\kappa)} \sqrt{w_{dev}(\omega_\kappa)}$$

3. Translating the distortion quantities in a multi-objective optimization problem

In the previous sections, two non-idealities have been quantified as object functions, namely the deviation w.r.t. a desired transfer function given by \hat{C}_{dev} , equation (8), and the distortion, given by $D\hat{S}R^2$:

$$D\hat{S}R^2 \equiv \sum_{\kappa} \frac{\hat{\sigma}_s^2(\kappa) + \hat{\sigma}_n^2(\kappa)}{\|U(\kappa)\|^2 \|\hat{G}_{BLA}(\kappa)\|^2} w_{dist}(\kappa) \quad (10)$$

with $w_{dist}(\kappa)$ being a weighting having the equivalent purpose as the weighting function in (8). Equation (10) can be written in an analogue way as (9), namely:

$$e_{DSR, \kappa} = \frac{\sqrt{\hat{\sigma}_s^2(\kappa) + \hat{\sigma}_n^2(\kappa)}}{\|U(\kappa)\| \|\hat{G}_{BLA}(\kappa)\|} \sqrt{w_{dist}(\kappa)}.$$

The distortion term $D\hat{S}R$ (Distortion-to-Signal Ratio) includes both the stochastic nonlinearities and the system noise, which represent two different distortion contributions in the same frequency band. Further, the distortion is defined as the inverse of the more common Signal-to-Distortion ratio. This is a reasonable choice since we chose that optimization means the minimization of the different object functions.

Both quantified non-idealities are then combined in a multi-objective cost function \hat{C}_{tot} :

$$\hat{C}_{tot} = \begin{bmatrix} D\hat{S}R^2 & \hat{C}_{dev} \end{bmatrix} \mathbf{w} \quad (11)$$

$$\text{with } \mathbf{w} = \begin{bmatrix} w_1 & w_2 \end{bmatrix}^T; w_1, w_2 \geq 0; w_1^2 + w_2^2 = 1$$

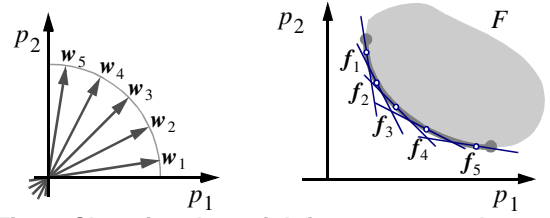


Fig. 4 Choosing the weighting vectors to determine the Pareto optimal front

Having determined this multi-objective cost function, an exploration of the performance space is carried out by minimizing (11) for different values of the weighting vector \mathbf{w} . Experimental results, described in section 4.2, show that choosing the weighting vectors uniformly distributed over the unit circle (illustrated in Fig. 4) allows to get a good idea of the Pareto optimal front. More sophisticated methodologies for determining the front have been elaborated, involving however more complicated algorithms [2]. For the optimization, note that (11) can be written as a sum of squares, giving the possibility to use the Levenberg-Marquardt algorithm [5], as described in section 3.1.

3.1. Practical implementation

An optimization can be performed by following one of the two following strategies. First, one could consider to carry out a performance space exploration for each building block and to extract a mathematical model for the Pareto optimal front and behavioral models for the building blocks. The models obtained can then be used in an optimization on the behavioral level [1]. The second strategy could be to perform an optimization w.r.t. a well-chosen parameter vector on behavioral level using circuit level simulations. In this case the circuit level parameters would be calculated using an automated design plan. A clear advantage of the first strategy is that it reduces significantly the needed simulation time when the behavioral level models are available, while the latter doesn't require a behavioral model of the building blocks. For this paper, the second strategy has been chosen.

The optimization uses the Levenberg-Marquardt algorithm in combination with a hierarchical designflow. To this end, a mathematical design plan has been set up in Matlab® to size the transistors of the building blocks (like the OTA's for a gm-C filter) in a hierarchical way. This design plan calculates the circuit level parameters of the building blocks as a function of some behavioral level design parameters (e.g. the g_m values and the bias current of the OTA's). The design parameters are then used as optimization parameters, denoted θ . It is clear that the choice of these parameters can be made in more than one way. It is however important to keep the number of optimization parameters small. Therefore a sensitivity study of the considered performances to these parameters was carried out prior to the optimization.

The optimization algorithm of Levenberg-Marquardt requires the cost function to be written as a sum of squares. This gives, in vector notation:

$$C(\theta) = e^T(\theta)e(\theta) \quad (12)$$

In this equation, $e^T(\theta)$ is the conjugate transpose of $e(\theta)$, which in turn is composed by stacking e_{dev} and e_{DSR} where real and imaginary parts have been separated and put below each other. The reason for this is to ensure that the results for the optimization parameters will be real. The algorithm then consists of taking a step δ of the optimization parameters. The step δ is computed by solving the following equation (parameter θ has been left out for convenience):

$$(J^T J + \lambda^2 I_{n_\theta})\delta = -J^T e \quad (13)$$

where λ is a non-negative real valued control parameter and where $J(\theta) = \frac{d}{d\theta}e(\theta)$ equals the Jacobian matrix. Since calculating the Jacobian analytically is not an obvious job, it is approximated by a numerical differentiation. A good starting value for λ is: $\lambda_{start} = \sigma_{max}(J)/100$ where $\sigma_{max}(J)$ is the greatest singular value of J . Note that calculating $J^T J$ explicitly in (13) is numerically unstable. Reference [5] discusses how to solve (13) without forming $J^T J$ explicitly.

The whole optimization algorithm can be summarized as follows:

1. Establish a design plan to size the building blocks and choose the optimization parameters such that a significant sensitivity of the performances to these parameters is observed.
2. Choose the starting values of the optimization parameters. These can be obtained from a classical design methodology and some insight in the circuits used.
3. Perform the transient and the noise analysis required to calculate the distortion and the deviation of the transfer function w.r.t. the desired characteristic and compute e and J .
4. Calculate a step δ for the optimization parameters from (13).
5. Compute a new value for λ and θ :

$$C(\theta + \delta) \geq C(\theta) \Rightarrow \lambda \rightarrow 10\lambda, \theta \text{ unchanged}$$

$$C(\theta + \delta) < C(\theta) \Rightarrow \lambda \rightarrow 0.4\lambda, \theta \rightarrow \theta + \delta$$
6. Check the convergence criterion. If it's not met, go back to step 3.

The Pareto optimal front can then be calculated by repeating this sequence for every weighting factor, chosen as explained in section 3. Note that the parameters obtained after one optimization with weighting vector w_i are good starting values for the optimization with the next weighting vector w_{i+1} .

4. Application on filter design

This section shows the results of the optimization applied on a filter in leapfrog configuration (section 4.1), the pareto optimal front obtained for a cascade of 2^{nd} order

sections (section 4.2) and a comparison between the nonlinear distortions of both configurations (section 4.3).

4.1. Results on leapfrog configuration

The optimization method described in section 3.1 has been applied to the design of a 6^{th} order Chebychev g_m -C filter in leapfrog configuration [6] in a 180nm technology. The results are illustrated in Fig. 5. The 'x' give the nonlinear-distortion-to-signal ratio before (green) and after (red) the optimization, calculated using (6). On this figure, one can observe:

- the smooth frequency dependency of the nonlinearities.
- a decrease of the nonlinear distortions of about 20dB.
- that the system noise ('o') does not change a lot. This is due to the fact that the nonlinearities are the dominating distortions in this case, hence making the optimization of the system noise superfluous.

This optimization was performed with eight tuning parameters (including six capacitor values, one transconductance and one overdrive voltage). The required computing time for one iteration of the optimization (involving 102 transient simulations of 6144 time points) was about 15 minutes. The final values were reached after about 20 iterations.

4.2. Pareto optimal front of a cascade of 2^{nd} order sections

An optimization has been carried out for different values of the weighting factors for a 6^{th} order Chebychev g_m -C filter composed of the cascade of 2^{nd} order sections. Fig. 6 shows the desired transfer function (black continuous line) and the BLA's (colored dots). The purple values were obtained when a higher weight was given to the distortions. A higher weight was given to the deviation of the transfer function for the blue values. The corresponding Pareto optimal front is illustrated in Fig. 7. When giving a high weight to the distortions, one can clearly observe the trade-offs which are made by lowering the transfer function, especially around the cut-off frequency. This can be explained by the fact that a cascade of 2^{nd} order sections will require some high quality factors of some sections around the cut-

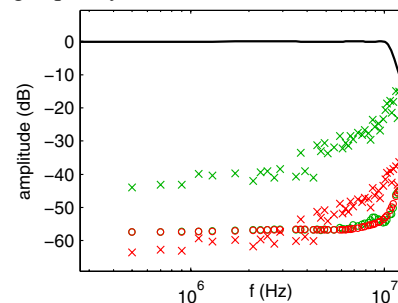


Fig. 5 Distortion before (green) and after (red) optimization; 'x': stochastic nonlinear distortion; 'o': system noise; ':' BLA

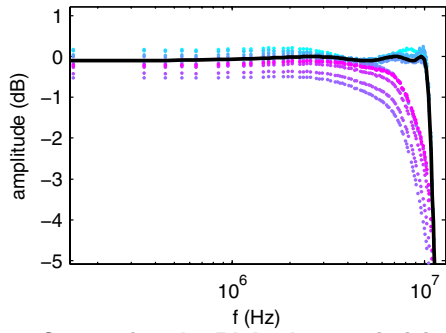


Fig. 6 Comparing the BLA when optimizing for several values for the weighting factors; ‘-’: desired transfer function; ‘•’: obtained BLA’s

off frequency, causing a higher peaking of the transfer function of these sections and generating more nonlinear distortions. Note that the trade-off allows the distortions to be reduced by a factor of almost four while the transfer function has not been harmed in a very significant way.

4.3. Comparing the two different filter topologies

Fig. 8 shows the nonlinearities for a leapfrog filter (top figure) and a cascade of second order sections (bottom figure) with both the same specifications and excitation signal (multisine with 50mV RMS and uniform power spectrum). The amplitude spectrum (dots) and the nonlinear distortions (circles) on the succeeding nodes (different colors) of the filters have been plotted. For the cascade, the last filter section (in magenta) seems to add a lot of nonlinearities to the signal, especially around the cut-off frequency. This isn’t the case for the leapfrog, where the levels of nonlinearities don’t increase from one node to the next. For this reason, allowing an important deviation around the cut-off frequency for this filter wouldn’t be as beneficial as was the case for the cascade. Nevertheless it seems that the leapfrog configuration shows a better linear behavior than the cascade.

5. Conclusions

This paper explains a methodology to quantify the nonlinear distortions of an active filter, such as to be comparable with the system noise. For this purpose the (weakly) nonlinear filter is modelled as a “Best Linear Approximation” with two noise contributions on the output signal, namely the system noise and the stochastic nonlinear contri-

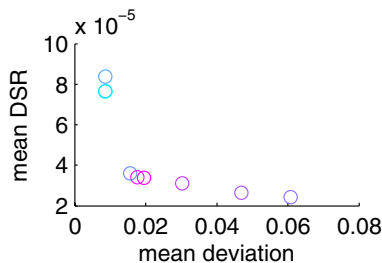


Fig. 7 Samples of the Pareto optimal front

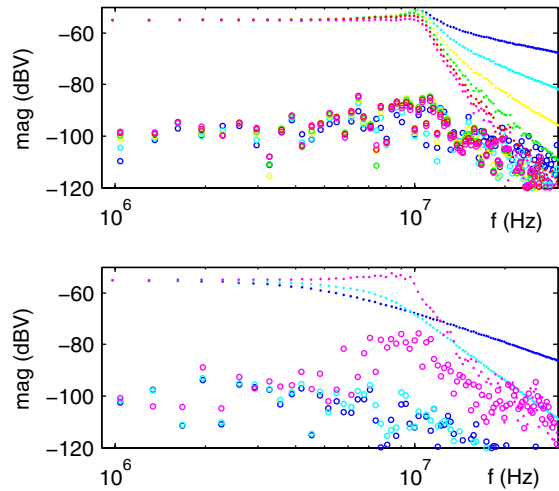


Fig. 8 Comparison of nonlinear distortions on succeeding nodes for a leapfrog configuration (a) and a cascade of 2nd order sections (b). ‘•’: amplitude spectrum; ‘o’: standard deviation of amplitude spectrum (nonlinear distortions)

butions. This method is applicable to the design of other circuits which are dominantly linear.

Having quantified the considered non-idealities (being the nonlinear distortions, the system noise and the deviation of the transfer function w.r.t. a desired characteristic), a multi-objective optimization of a filter design was carried out. It has been shown that, for a cascade of 2nd order sections, a significant trade-off can be made between distortions and the deviation of the transfer function.

The nonlinear distortions of a leapfrog filter and a cascade have been compared. It was shown that the former has a better ability to oppress the nonlinearities than the latter.

6. References

- [1] J. Zou, D. Mueller, H. Graeb and U. Schlichtmann (2006) - *A CPPLL Hierarchical Optimization Methodology Considering Jitter, Power and Locking Time* - DAC 2006, pp 19-24
- [2] D. Mueller, G. Stehr, H. Graeb and U. Schlichtmann (2005) - *Deterministic Approaches to Analog Performance Space Exploration (PSE)* - DAC 2005, pp 869-874
- [3] Schoukens J., T. Dobrowiecki and R. Pintelon (1998) - *Parametric Identification of Linear Systems in the Presence of Nonlinear Distortions. A Frequency Domain Approach* - IEEE Trans. Autom. Contr., vol. AC-43, no.2, pp. 176-190.
- [4] L. De Locht, G. Vandersteen, P. Wambacq, Y. Rolain, R. Pintelon, J. Schoukens, and S. Donnay - *Identifying the main nonlinear contributions: use of multisine excitations during circuit design* - ARFTG Microwave Measurements Conference, Orlando, FL, USA, pp. 75-84, 2004.
- [5] Fletcher R. (1987) - *Practical Methods of Optimization* - Wiley & Sons
- [6] Deliyannis, Theodore L. et al “Frontmatter” - *Continuous-Time Active Filter Design* - Boca Raton: CRC Press LLC, 1999